

 **ITINERIS**

D4.14.3 Documentation of developed data products capable of providing information on air quality in relation to the atmospheric stratification and dynamics. [B17]



Deliverable number:	D4.14.3
Work package:	WP4 – Atmosphere
Intermediate Objective:	IO 4.7
Deliverable type:	<input checked="" type="checkbox"/> Document, report
	<input type="checkbox"/> Websites, patent filings, videos, etc.
	<input type="checkbox"/> Other: please specify
Dissemination level:	<input checked="" type="checkbox"/> Public
	<input type="checkbox"/> Restricted
Estimated delivery (bimester):	B15
Actual delivery date:	31 August 2025
Author(s) (Partner-OU):	Marco Zanatta, Camilla Perfetti, Francesca Barnaba, Alessandro Bracci, Luca Di Liberto, Angela Marinoni, Simonetta Montaguti, Ferdinando Pasqualini, Paolo Pettinari, Marco Rapuano, Laura Renzi, Nora Zannoni (CNR-ISAC)
Reviewed by:	Lucia Mona, Gianluca Di Fiore (CNR-IMAA)
Note:	

IR0000032 – ITINERIS, Italian Integrated Environmental Research Infrastructures System -
CUP B53C22002150006 (D.D. n. 130/2022)

Funded by EU - Next Generation EU

Mission 4 “Education and Research” - Component 2: “From research to business” -

Investment 3.1: “Fund for the realisation of an integrated system of research and innovation infrastructures”

Table of contents

<i>1</i>	<i>INTRODUCTION</i>	<i>6</i>
<i>2</i>	<i>FIELD OBSERVATIONS</i>	<i>6</i>
2.1	RI-URBANS	6
2.1.1	Site description.....	7
2.1.2	Instrumental set-up and data coverage.....	7
2.2	Mt. Cimone long-term observations	8
2.2.1	Site and representativity.....	8
2.2.2	Instrumental set-up and data coverage.....	9
2.2.3	Reanalysis and modelling data.....	10
<i>3</i>	<i>DESCRIPTION OF DATA PRODUCTS</i>	<i>11</i>
3.1	Air quality and boundary layer in Milan	11
3.1.1	Air quality dataset.....	11
3.1.2	Proxy for planetary boundary layer height	12
3.2	Black carbon, boundary layer and sources at Mt.Cimone	13
3.2.1	From ACTRIS L0 data to ITINERIS L3 product	14
3.2.2	Planetary boundary layer height from reanalysis.....	15
<i>4</i>	<i>DATA AVAILABILITY</i>	<i>16</i>
<i>5</i>	<i>IMPACT OF ATMOSPHERIC DYNAMICS ON AIR QUALITY</i>	<i>17</i>
5.1	Efficient summer dilution in the Po Valley	17
5.2	Export of pollution at high altitude	19

List of figures

Figure 1: Left panel: location of the city of Milan in Italy; right panel: map of the city with the position of the four measurements stations.....	7
Figure 3 Temporal data coverage of the remote and in-situ observations performed at Milan during the RIURBANS campaign in 2023.	8
Figure 4 Availability of equivalent black carbon data at the Cimone observatory between 2007 and 2022.....	10
Figure 5 Time series of eBC carbon mass concentration (derived from absorption coefficients measured at 880 nm wavelength) at the hot-spot site.	12
Figure 6 a) Example of CHM-15k level 1 data measured at Milano Bicocca over 24 hours in April 2023. b) Time series of Level 3 product, mixed aerosol layer height derived from backscattering profiles during the full RI-URBANS campaign.	13
Figure 7 Integration of long-term observations performed at Cimone with Copernicus and FLEXPART products.....	14
Figure 8 Processing scheme from level 0 to level 3 applied to MAAP data acquired at Cimone Station.....	15
Figure 9 Diel variability of mixed aerosol layer, eBC mass concentration and total particle number concentration in winter (top) and summer (bottom) 2023 in Milan.	17
Figure 10 Example of correlation of the mixed aerosol layer height with equivalent black carbon mass concentration and with total particle number concentration in winter (top) and summer (bottom).....	18
Figure 11 Monthly time series of: the equivalent black carbon mass concentration (eBC) measured at Cimone Station; height of the planetary boundary layer (PBLH) derived from ERA5 reanalysis data over the Po Valley.	19
Figure 12 Seasonal cycle of the equivalent black carbon mass concentration (eBC) measured at Cimone Station; height of the planetary boundary layer (PBLH) derived from ERA5 reanalysis data over the Po Valley.	20
Figure 13 Correlation between the observed equivalent black carbon mass concentration and height of the planetary boundary layer at the Cimone observatory.	21

1 INTRODUCTION

Atmospheric aerosols and gases, originating from both natural and anthropogenic sources, play a crucial role in Earth's climate, air quality, and human health. They influence the planetary energy balance by scattering and absorbing solar and infrared radiation and have significant implications for air quality, with direct health effects. Despite extensive research, major uncertainties remain regarding the factors controlling the concentration and distribution of aerosols and gases across different atmospheric layers.

A key factor influencing pollution dispersion is the Planetary Boundary Layer (PBL), the lowest part of the atmosphere that directly interacts with the Earth's surface. The PBL controls the mixing and vertical transport of pollutants, with its height and structure varying due to meteorological conditions, surface properties, and local emission sources. Seasonal changes in the PBL significantly impact air quality; for example, a shallow PBL during winter can trap pollutants near the surface, while a deeper PBL in summer facilitates their dispersion. Additionally, complex interactions with urban heat islands, wind patterns, and extreme weather events can further modulate pollutant concentrations.

Given these dynamics, improving our ability to characterize the PBL and its role in pollutant dispersion is critical for air quality assessment and mitigation strategies. The ITINERIS project addresses this challenge by integrating ceilometer-based remote sensing with in-situ observations and reanalysis data, generating a comprehensive observational dataset to evaluate PBL evolution and its influence on aerosol and trace gas concentrations.

This deliverable focuses on the documentation of the data products developed within the ITINERIS project to provide insight into air quality in relation to atmospheric stratification and dynamics. Specifically, it presents the structure, content, and applications of the data products generated from the RI-URBANS (Research Infrastructures Services Reinforcing Air Quality Monitoring Capacities in European Urban & Industrial Areas. G.A. 101036245) campaign in Milan and the ACTRIS (Aerosol, Clouds and Trace Gases Research Infrastructure) observational activities at Monte Cimone.

These activities underscore the importance of integrating remote sensing with in-situ and reanalysis data. The documented data products represent a foundational resource for advancing our understanding of atmospheric processes and for supporting further research, forecasting, and policy applications.

2 FIELD OBSERVATIONS

2.1 RI-URBANS

A comprehensive one-year measurement campaign (2023) in Milan was conducted within the framework of the RI-URBANS project. Milan is the second-largest city in Italy and, due to the poor air circulation in the Po Valley, is prone to poor air quality. As one of the 13 European pilot cities of RI-URBANS, Milan was chosen for its strategic relevance in understanding urban air pollution dynamics.

2.1.1 Site description

The campaign integrated in-situ and remote sensing observations across four key measurement sites, designed to characterize air quality, aerosol properties, and atmospheric stratification (**Error! Reference source not found.**). The two primary in-situ sites were:

- Milan-CNR (urban background station) – Representing typical urban pollution levels.
- Milan-Linate airport (urban hotspot site) – A high-emission area near intense traffic and airport operations.



Figure 1: Left panel: location of the city of Milan in Italy; right panel: map of the city with the position of the four measurements stations.

2.1.2 Instrumental set-up and data coverage

At Milan-Linate, the AEROLAB (AERosol mObile LABORatory) platform, an ACTRIS-RI exploratory unit, was deployed from January to September 2023 (Figure 2). It conducted continuous measurements of aerosol optical properties (absorption, scattering, backscattering), aerosol size distributions from 10 nm to 20 μm , covering both ultrafine and coarse particles, trace gas concentrations (NO , NO_2 , NO_x) and meteorological parameters, including wind, temperature, pressure, and radiation. Simultaneously, the Voyager3 laboratory, located at Milan-CNR, provided an advanced suite of instruments for online aerosol chemical composition (ToF-ACSM), volatile organic compounds (VOCs) analysis using a VOCUS CI-ToF (Chemical Ionization Time of Flight Mass Spectrometer equipped with a Vocus reactor) and greenhouse gas monitoring (CO_2 , CH_4 , H_2O) with a Picarro analyzer. Although most analyses focused on Linate, the CNR site served as a reference for urban background conditions, enabling comparisons between hotspot emissions and typical urban air masses. In addition to in-situ measurements, lidar-based aerosol remote sensing measurements were performed at university of Milan-Bicocca and Rubattino Station. These

sites hosted two ceilometers as part of the ALICENET (Automated Lidar-Ceilometer network) network: CHM15k (Lufft) at Bicocca, operating January–September 2023, CL61 (Vaisala) at Rubattino, operational since June 2023, with depolarization capability useful for aerosol typing. Ceilometer data provided continuous profiling of aerosol attenuated backscatter, essential for determining the mixed aerosol layer (MAL), a key indicator of planetary boundary layer (PBL) height.

This campaign represents the most extensive and detailed atmospheric observation effort in Milan to date. By integrating in-situ and remote sensing data, it enables a multi-dimensional analysis of urban air pollution, boundary layer dynamics, and aerosol interactions.

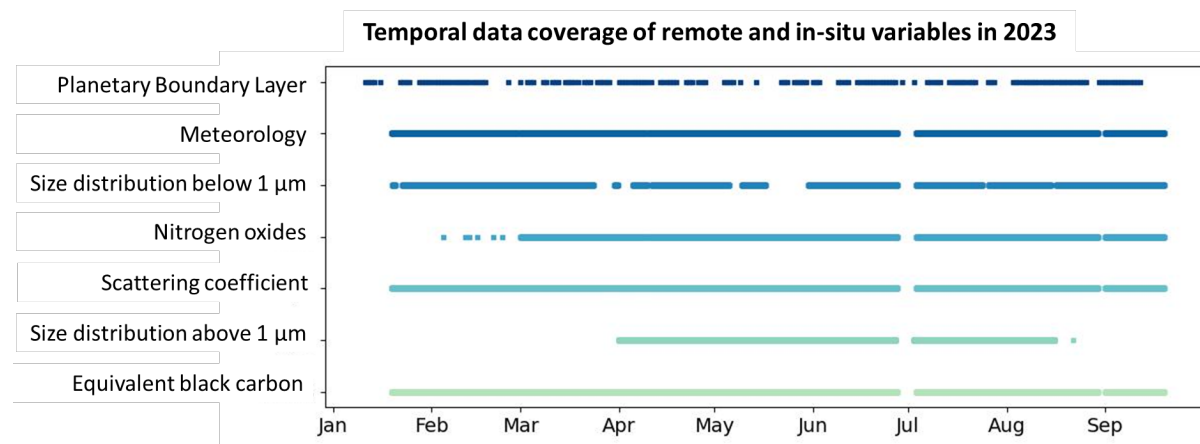


Figure 2 Temporal data coverage of the remote and in-situ observations performed at Milan during the RIURBANS campaign in 2023.

2.2 Mt. Cimone long-term observations

The “Ottavio Vittori Observatory” on the top of Mt. Cimone (CMN, 44°12’ N, 10°42’ E). Is supervised by the Institute of Atmospheric Sciences and Climate (CNR-ISAC) of Bologna. With an elevation of 2165 m asl, CMN is representative of background conditions of the Mediterranean troposphere while being influenced by Mediterranean aerosol anomalies including dust outbreaks, forest fires, anthropogenic pollution and sea spray advection (Cristofanelli et al., 2018). CMN is the only Global Station of the Global Atmosphere Watch present on the Italian territory and contributes to ACTRIS-RI (Aerosol, Clouds, Trace Gases Research Infrastructure) and ICOS-RI (Integrated Carbon Observation System) managed within ESFRI (European Strategy Forum on Research Infrastructures). Hence, CMN contributes regularly to the European-scale studies, being included in 143 peer-reviewed publications since 1993.

2.2.1 Site and representativity

Considering the limited presence of anthropogenic emissions in the direct vicinity of the observatory, CMN may be considered as representative of the free-tropospheric atmospheric background, with daily-seasonal influence from the polluted boundary layer intrusion, and episodic influence of anthropogenic and natural pollution events. As a matter of fact, during the warmer seasons several aerosol classes such as anthropogenic pollution, mineral dust

and sea salt may be identified (Marenco et al., 2006). From spring to autumn the diurnal growth of the planetary boundary layer and the thermal wind system causes an efficient export of pollution from the polluted boundary layer to the CMN during the day time as observed from ozone, carbon monoxide and water-vapor measurements (Cristofanelli et al., 2009, 2015) and black carbon and aerosol particle measurements (Marinoni et al., 2008). The influence from the polluted boundary layer thus decreases during night and in winter, when an almost null diurnal variability is observed. With increasing temperature in the mediterranean, heat waves and aridification are expected to increase in the near future (MedECC, 2020). First, advection of pollutants and photo production of ozone are enhanced during heatwaves events (Cristofanelli et al. 2007). Second, aridification might lead to an increasing frequency of biomass burning events and subsequent emissions, which are traced with a combination of ozone and carbon monoxide measurements and back-trajectory analysis (Cristofanelli et al., 2009, 2013) and found to occur preferentially during the warmer part of the year, from May till September, and have a global, regional or local origin. As a consequence of increasing desertification in the Mediterranean Basin, the occurrence and severity of dust storm in southern Europe is expected to increase in the future decades (MedECC, 2020). CMN lays on the northern transport pathway of Saharan mineral dust from Northern Africa to Europe (Israelevich et al., 2012) and it is periodically affected by dust outbreaks originating from northern western and central Africa, from where the transport is particularly efficient during the warmer periods from spring to autumn, dominating the coarse aerosol particle number concentration (Duchi et al., 2016).

2.2.2 Instrumental set-up and data coverage

Among the long-term observations, special focus is given to the measurement of aerosol absorption coefficient using the Multi-Angle Absorption Photometer (MAAP). These measurements, covering the period 2007–2024, provide one of the longest continuous time series of aerosol light absorption in Southern Europe. Most of the measurements covers, at least, 6 months per year, with the highest data coverage recorded in 2014-15 and 2017-2019 (Figure 3). From MAAP data, the equivalent black carbon (eBC) concentrations were derived, offering crucial insights into the variability and long-term trends of light-absorbing aerosols at high altitude.

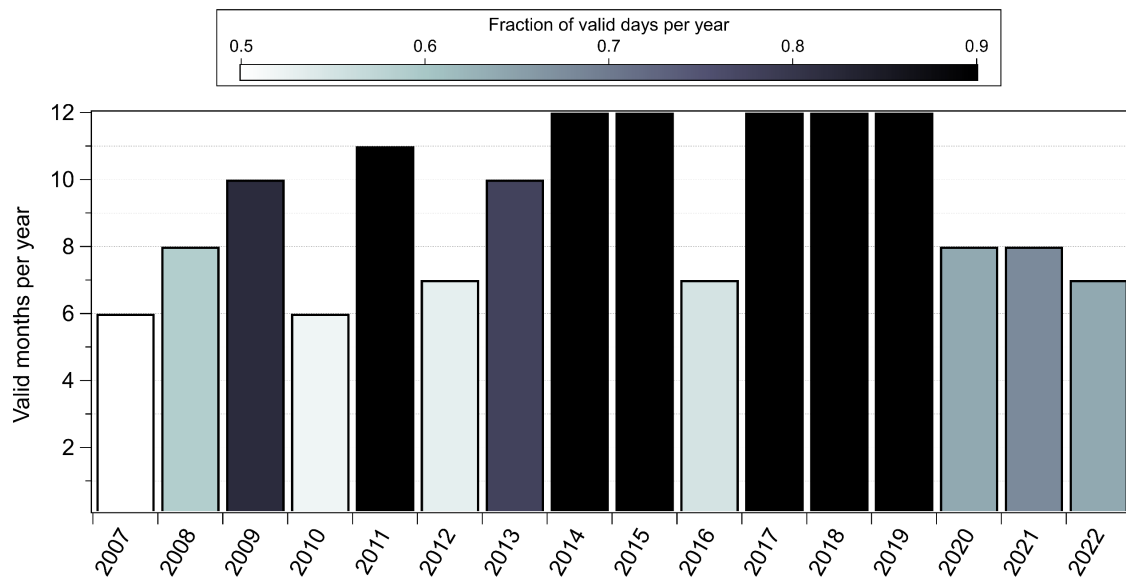


Figure 3 Availability of equivalent black carbon data at the Cimone observatory between 2007 and 2022.

2.2.3 Reanalysis and modelling data

To understand the seasonal impact of the boundary layer dynamics on BC concentration at CMN, we integrated data from reanalysis and modeling tools with in-situ observations over the period 2007–2023. The ERA5 reanalysis was used to extract the planetary boundary layer (PBL) height, providing insight into the site’s coupling with boundary layer dynamics and its exposure to Po Valley emissions. These global georeferenced reanalysis data are available with a $0.25^{\circ} \times 0.25^{\circ}$ horizontal resolution and a pressure range of 1000 -1 hPa binned on 37 pressure levels. A detailed description of the ERA5 products is provided by Hersbach et al. (2020). CAMS global reanalysis data were employed to retrieve BC concentration at regional scale, enabling the characterization of large-scale patterns and long-range transport events. These global georeferenced reanalysis data (fourth generation ECMWF global reanalysis; EAC5) are available with a $0.75^{\circ} \times 0.75^{\circ}$ horizontal resolution and a pressure range of 1000 -1 hPa binned on 25 pressure levels. An overview of the CAMS products is provided by Inness et al. (2019), while details on the aerosol schemes are given in Morcrette et al. (2009) and Bozzo et al. (2017). Additionally, the FLEXPART Lagrangian dispersion model was applied to determine the source region and emission type of the air masses reaching the site, distinguishing between anthropogenic and natural contributions to black carbon aerosol (Pisso et al., 2019). Domestic sources are defined as residential and commercial sectors including emissions from combustion in heating and cooking stoves and boilers in households, and public and commercial buildings. Transportation includes emissions from all land-based transport of goods, animals and persons on road networks and off-road activities. Forest fire contribution represents open biomass burning (excluding agricultural fires) and accounts, only, for natural emissions. This combined approach allowed for a more robust interpretation of the observed aerosol variability at CMN, particularly regarding the roles of PBL dynamics, free-tropospheric influence, and Po Valley outflow.

3 DESCRIPTION OF DATA PRODUCTS

3.1 Air quality and boundary layer in Milan

In this part of the work, we describe the full data treatment procedure necessary to derive the data products at Milan, involving in-situ observations and remote sensing.

3.1.1 Air quality dataset

For the RI-URBANS project, various air quality metrics have been assessed from the aerosol phase within PM₁. PM₁ refers to particulate matter with a diameter of less than 1 micron (1 μm). These fine particles are a subset of PM_{2.5} and are primarily generated from combustion sources such as vehicle emissions, industrial activities, biomass burning, and secondary aerosol formation. Due to their small size, PM₁ particles can penetrate deep into the respiratory tract and even enter the bloodstream, posing significant health risks, including cardiovascular and respiratory diseases. Currently, there are no specific EU air quality limit values or guidelines set for PM₁. However, PM₁ is increasingly being measured and considered in scientific research and policy discussions due to its relevance for human health and its potential to support more targeted air quality mitigation strategies. One of the major components of PM₁ considered in this deliverable is the equivalent black carbon (eBC) mass concentration. In Milan, eBC was derived from the aerosol absorption coefficient measured at a wavelength of 880 nm using an aethalometer (model AE33). The conversion to eBC mass concentration was carried out assuming a mass absorption cross-section (MAC) of 7.8 m^2/g .

The time series used in this analysis covers the period from 19/01/2023 to 19/09/2023 and exhibits a characteristic seasonal cycle, with higher concentrations observed in winter and lower levels in summer (Figure 4). Other important measured metrics include the total particle number concentration and the contribution of different size modes—namely nucleation, Aitken, and accumulation—to the total aerosol number concentration below 1 μm . Within RI-URBANS, PM₁ mass concentration was not measured directly but was instead estimated from the aerosol number size distribution, which was measured using a Scanning Mobility Particle Sizer (SMPS-TROPOS), assuming a constant particle density of 1.5 g/cm^3 . Additional gaseous pollutants measured during the campaign include nitrogen oxides (NO and NO₂), which are key indicators of traffic-related emissions and important precursors to secondary aerosol formation. In addition to NO_x, VOC were measured simultaneously in real time during every season at an urban background site. Volatile organic compounds are thousands of reactive trace gases directly emitted from a variety of sources, including traffic and natural sources as well as generated from oxidation reactions occurring in the troposphere. Their nature of primary and secondary pollutant makes them particularly relevant when measured together with the PBL. Benzene is the only VOC considered in the EU air quality standards.

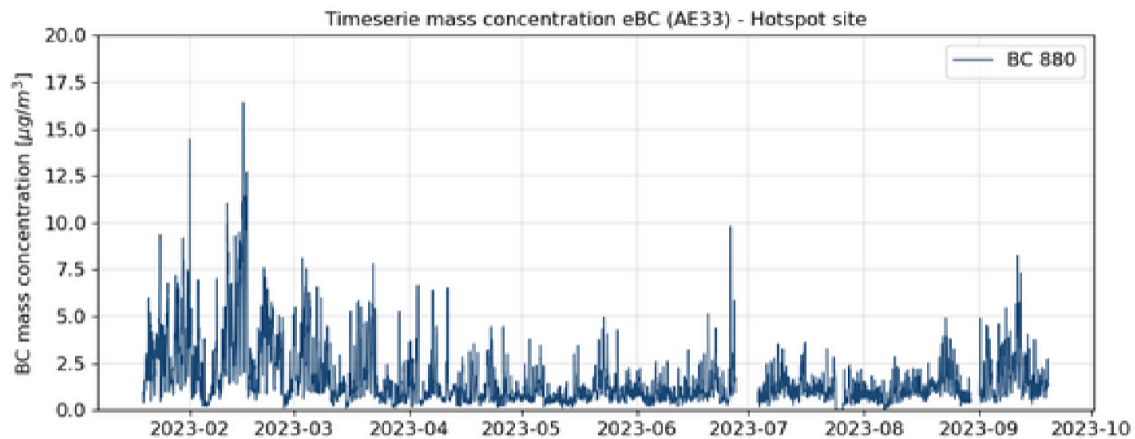


Figure 4 Time series of eBC carbon mass concentration (derived from absorption coefficients measured at 880 nm wavelength) at the hot-spot site.

3.1.2 Proxy for planetary boundary layer height

This chapter presents the RIURBANS dataset derived from continuous lidar-ceilometer observations at the Remote site 1 (**Error! Reference source not found.**). The CHM15k is a vertically pointing, single-wavelength lidar-ceilometer that operates at 1064 nm in the near-infrared range. It is designed for continuous, unattended atmospheric monitoring and provides high-resolution measurements of the backscattered signal from atmospheric constituents such as aerosols and clouds. The instrument directly measures the intensity of the backscattered light as a function of altitude and time, producing range-corrected backscatter profiles as Level 1 data (Figure 5a). These profiles are used to detect cloud base heights and to infer aerosol layer structures. While the CHM15k does not directly measure aerosol mass concentrations or boundary layer height, it provides the raw optical backscatter data needed for advanced retrieval algorithms—such as ALADIN (Bellini et al., 2024, 2025) to estimate the mixed layer height and identify elevated aerosol layers. A central algorithm named ALADIN processes the attenuated backscatter profiles to detect aerosol layers. It identifies the Mixed Aerosol Layer (MAL, Figure 5b), which represents the turbulent, well-mixed near-surface layer and is analogous to the planetary boundary layer (PBL). Additionally, ALADIN detects Continuous Aerosol Layers (CAL) and Elevated Aerosol Layers (EALs), which are more vertically extended or located above the ground. The algorithm determines these layers by analyzing correlations within the backscatter profiles, allowing for the estimation of layer heights and depths in near real time. These Level 2 data products are used to infer the relationship between air pollutants and atmospheric dynamics.

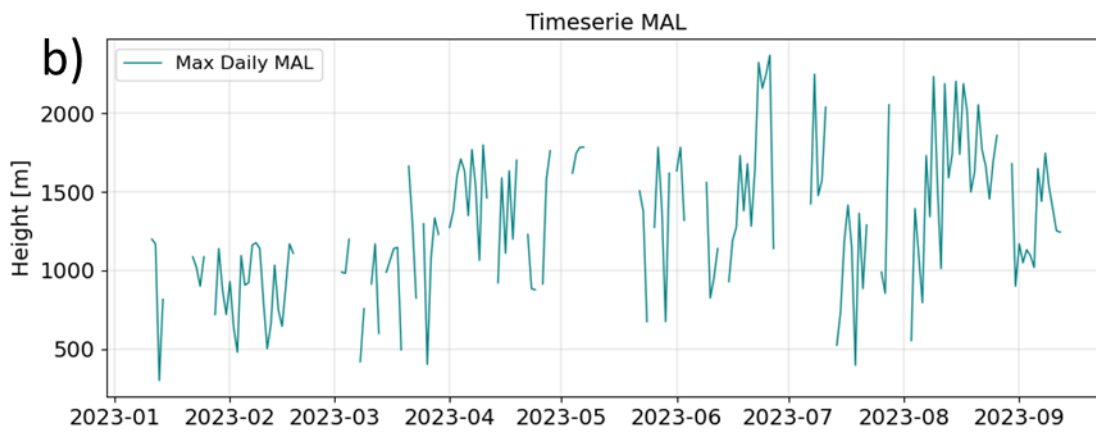
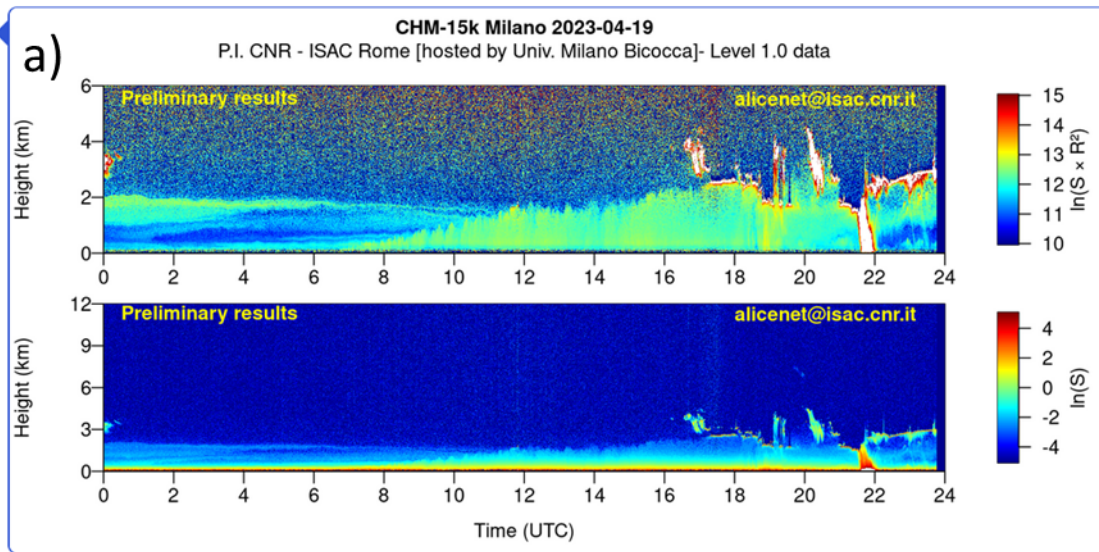


Figure 5 a) Example of CHM-15k level 1 data measured at Milano Bicocca over 24 hours in April 2023. b) Time series of Level 3 product, mixed aerosol layer height derived from backscattering profiles during the full RI-URBANS campaign.

3.2 Black carbon, boundary layer and sources at Mt.Cimone

In this part of the work, we describe the full data treatment procedure necessary to derive the data products at Cimone, involving in-situ observations, reanalysis and modelling as shown in Figure 6.

Integration of long-term observations with numerical simulation at Mt.Cimone

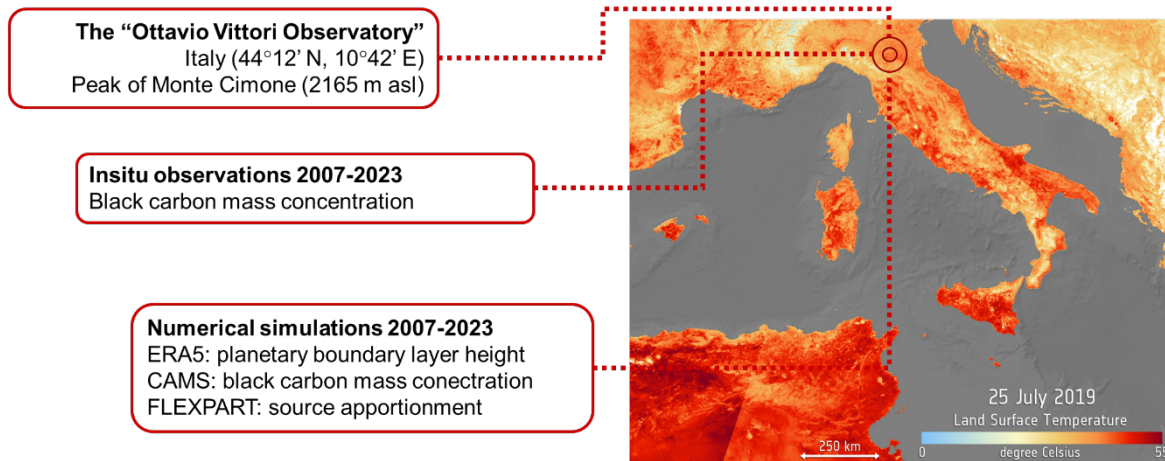


Figure 6 Integration of long-term observations performed at Cimone with Copernicus and FLEXPART products

3.2.1 From ACTRIS L0 data to ITINERIS L3 product

The first data reduction step involves identifying and addressing mechanical and signal anomalies to produce Level 0 data, in line with the ACTRIS guidelines. The temporal resolution of Level 0 data is one minute. Mechanical anomalies were primarily related to the sampling flow rate, in addition to routine filter spot changes and zeroing tests indicated by the instrument status. The standard sampling flow rate for the MAAP is 16.7 lpm. Periods with a sampling flow rate between 6 lpm and 8.3 lpm were included only after additional inspection and labelled and to be considered as valid but irregular. Periods with flow rates below 6 lpm are subject to variability up to 13% (Müller et al., 2011), and were excluded. Data points with standard deviation of sample flow greater than 5% over a 5-minute time window were also removed. Periods with a sampling flow rate above 18 lpm were considered valid only if the relative standard deviation was below 5%, and no anomalies were detected in the black carbon concentration or filter load. These periods were flagged using the value 110, indicating episode data checked and accepted by the data originator, as recommended by ACTRIS. Signal anomalies were identified by evaluating the variability of the raw BC mass concentration data provided by the MAAP at a 1-minute resolution. In alignment with ACTRIS guidelines, noise around or below zero is expected at a 1-minute resolution near the detection limit. However, negative values are unphysical in hourly averages and must be considered invalid. To identify these events, a "noise filter" was applied to remove data points associated with negative values in a one-hour rolling average (± 30 minutes from the considered point). To further identify periods affected by high variability, a rolling 5th and 95th percentile (P05 and P95) was calculated within a one-hour time window (± 30 minutes). Data points showing simultaneous negative P05 values and a difference between P95 and P05 exceeding $1 \mu\text{g m}^{-3}$ were flagged as divergent data and filtered out. Remaining data points were visually inspected for consistency and flagged as valid if no further anomalies were detected. The second step of the data reduction process aims to convert the eBC mass concentration into aerosol absorption coefficient, correct the instrumental errors and adjust

the resulting atmospheric variable to standard pressure and temperature. First, eBC mass concentration obtained in L0 was converted in aerosol absorption coefficient at a wavelength of 670 nm (abs_{670}^{L1}) applying the mass absorption cross-section used in the MAAP firmware ($6.6 \text{ m}^2 \text{ g}^{-1}$; Slowik et al., 2007). In order to account for the inaccuracy of the optical wavelength of MAAP, having an actual wavelength of 637 nm instead of a nominal wavelength of 670 nm, the aerosol absorption coefficient was adjusted with a multiplication factor of 1.05 (Müller et al., 2011). Finally, the resulting aerosol absorption coefficient at a wavelength of 637 nm was adjusted to standard pressure (113.25 hPa) and temperature (273.15 K) using the pressure and temperature measured in the sampling line. The most substantial change from Level 1 to Level 2 data is the change in the data time stamp. All instrumental variables such as temperature, pressure and relative humidity were averaged over one our time stamp. Equivalent black carbon mass concentration (Level 3) is calculated from the aerosol absorption coefficient (L2) by means of the mass absorption cross section (MAC) as: $M_{eBC} = \sigma_{ap637}/MAC_{637}$. A MAC value of $10 \text{ m}^2 \text{ g}^{-1}$, representative of European background conditions (Zanatta et al., 2016), was used for the conversion. Statics were calculated over one hour time stamp. For the present work, data were averaged on monthly base.

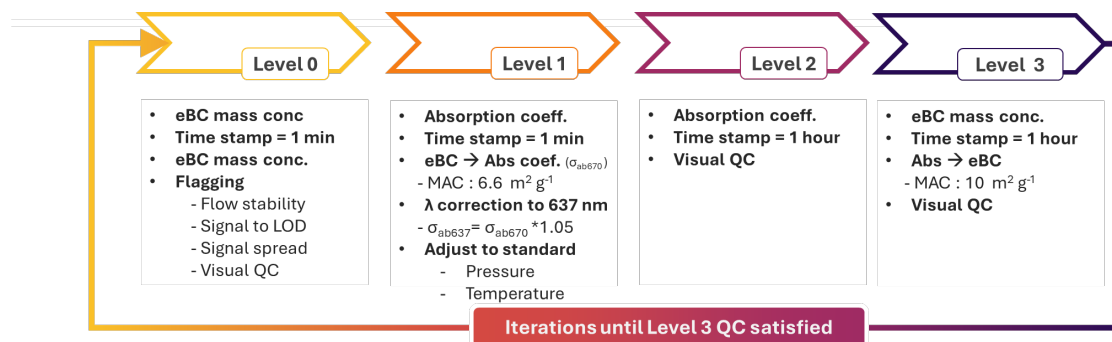


Figure 7 Processing scheme from level 0 to level 3 applied to MAAP data acquired at Cimone Station.

3.2.2 Planetary boundary layer heigh from reanalysis

To understand the seasonal impact of the boundary layer dynamics on BC concentration at CMN, we integrated data from reanalysis and modeling tools with in-situ observations over the period 2007–2023. ERA5 is a global climate reanalysis dataset produced by the European Centre for Medium-Range Weather Forecasts (ECMWF) under the Copernicus Climate Change Service (C3S). It provides hourly estimates of a large number of atmospheric, land, and oceanic climate variables from 1950 to present, using a combination of model data and observations. A detailed description of the ERA5 products is provided by Hersbach et al. (2020).

For the present deliverable, we used the “ERA5 hourly data on single levels from 1940 to present” dataset, which is available at a $0.25^\circ \times 0.25^\circ$ horizontal resolution. It provides data over a pressure range of 1000 to 1 hPa, binned across 37 pressure levels (DOI: 10.24381/cds.adbb2d47).

The region of interest includes three sectors representative of the Po Valley, located near the Cimone station:

- Piacenza sector: 45.50–45.00°N, 10–9°E
- Parma sector: 45.25–44.75°N, 11–10°E
- Bologna sector: 45.00–44.50°N, 12–11°E

The temporal coverage matches the availability of MAAP data. The ERA5 variable BLH was identified as a key parameter. BLH represents the depth of the atmosphere most influenced by surface-induced turbulence and resistance to the transfer of momentum, heat, and moisture. It can range from a few tens of metres (e.g., during nocturnal cooling) to several kilometres (e.g., over deserts on hot sunny days). When the boundary layer is shallow, pollutants emitted at the surface tend to accumulate near the ground. In ERA5, BLH is calculated using the bulk Richardson number, which reflects atmospheric stability conditions, in line with the conclusions of a 2012 review. For this analysis, the three sectors were merged and treated as a single region of interest (ROI). To derive the maximum altitude of the planetary boundary layer (PBL), the daily maximum BLH was computed over the ROI. The data were then aggregated to a monthly time resolution to align with in-situ observations. As such, the PBL height reported here represents the monthly average of the daily maximum values.

4 DATA AVAILABILITY

The data presented in this deliverable are publicly available on various data portals. The aerosol in-situ Level 2 data acquired during the RI-URBANS campaign held in Milan in 2023 are available at the NILU data portal (<https://ebas-data.nilu.no/>). These data are listed under the facility name “Milano Linate Airport” and the framework “RI-URBANS”. Level 2 data of 16 VOCs with different origin and atmospheric reactivity are under submission on the NILU data portal (<https://ebas-data.nilu.no/>). Some of these compounds (i.e. D4 and D5, recently reported to be emergent pollutants in the US) are reported for the first time in Europe. Level 1 data of the aerosol backscattering coefficient measured by the CHM15k ceilometer can be viewed on the ALICENET portal under the site name “Milan” (<https://www.alice-net.eu/>) and are available upon request. Regarding the Cimone observations, aerosol absorption coefficient data are available on the NILU portal under the facility name “Monte Cimone”, with the instrument listed as “filter_absorption_photometer” and the component name “aerosol_absorption_coefficient”. PBL height derived from ERA5 reanalysis is available through the Copernicus Climate Data Store (<https://cds.climate.copernicus.eu/>) under the variable name “Boundary layer height” (DOI: 10.24381/cds.adbb2d47).

Within the scope of the ITINERIS project, the data products related to the RI-URBANS and Monte Cimone observations presented in this deliverable will be published in the data repository available through the ITINERIS-HUB (<https://hub.itineris.cnr.it/datasets/>).

5 IMPACT OF ATMOSPHERIC DYNAMICS ON AIR QUALITY

5.1 Efficient summer dilution in the Po Valley

The in-situ and remote sensing data on one hour time resolution were organized to study the daily cycle in different seasons. Both the height of the boundary layer and the concentration of atmospheric pollutants have a clear daily variability, which may be more or less pronounced in winter or in summer (Figure 8). The mixed aerosol layer (MAL) height showed a marked increase and deeper development in summer compared to winter, with a peak occurring in the late morning and early afternoon due to efficient convective processes driven by solar irradiation. The marker for primary anthropogenic emissions, eBC, exhibited an opposite diurnal pattern, characterized by two peaks during rush hours. This cycle was prominent in winter and less evident in summer, when median concentrations remained well below $1 \mu\text{g m}^{-3}$. It is interesting to note how the diurnal variation of total particle number concentration changed from winter to summer. In summer, the typical rush hour pattern disappeared, suggesting the presence of other emission sources, potentially of secondary origin. The marked decrease of aerosol concentration from winter to summer is firstly associated with the decrease of emission, but the contribution of vertical dilution caused by a deep development of the MAL cannot be ignored.

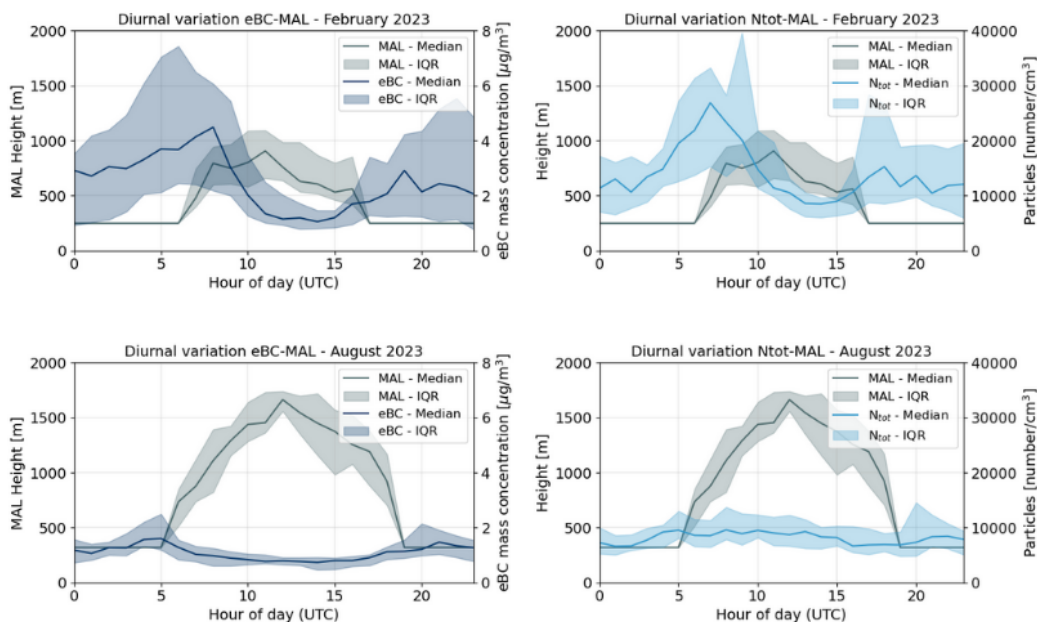


Figure 8 Daily variability of mixed aerosol layer, eBC mass concentration and total particle number concentration in winter (top) and summer (bottom) 2023 in Milan.

Thanks to these data products, we performed a correlation study between the MAL height and ground-level pollutant concentrations. The objective was to derive seasonal correlation coefficients between MAL height and aerosol concentration, in order to better understand

the relationship between vertical dilution and surface-level pollution. Hourly median values were averaged on a monthly basis and plotted as scatter plots in Figure 9.

In winter, aerosol concentration variability appears to be driven by factors other than atmospheric dynamics, as indicated by the absence of correlation—or even a weak anticorrelation—between MAL height and pollutant levels. In contrast, during summer, the diurnal development of the MAL, combined with reduced emissions, seems to be the dominant factor influencing the concentration of primary pollutants such as eBC. In this season, eBC mass concentrations are clearly and strongly anticorrelated with MAL height, showing a pronounced linear relationship. The relationship between MAL height and total particle number concentration is different, as it may be influenced by both primary emissions and secondary formation processes. In this case, a slightly positive correlation is observed, though with a large degree of variability, suggesting the interplay of competing effects between dilution and new particle formation. Future work may extend this analysis to VOC of primary, secondary and mixed origin in order to help assessing the identity of the measured compound by using MAL.

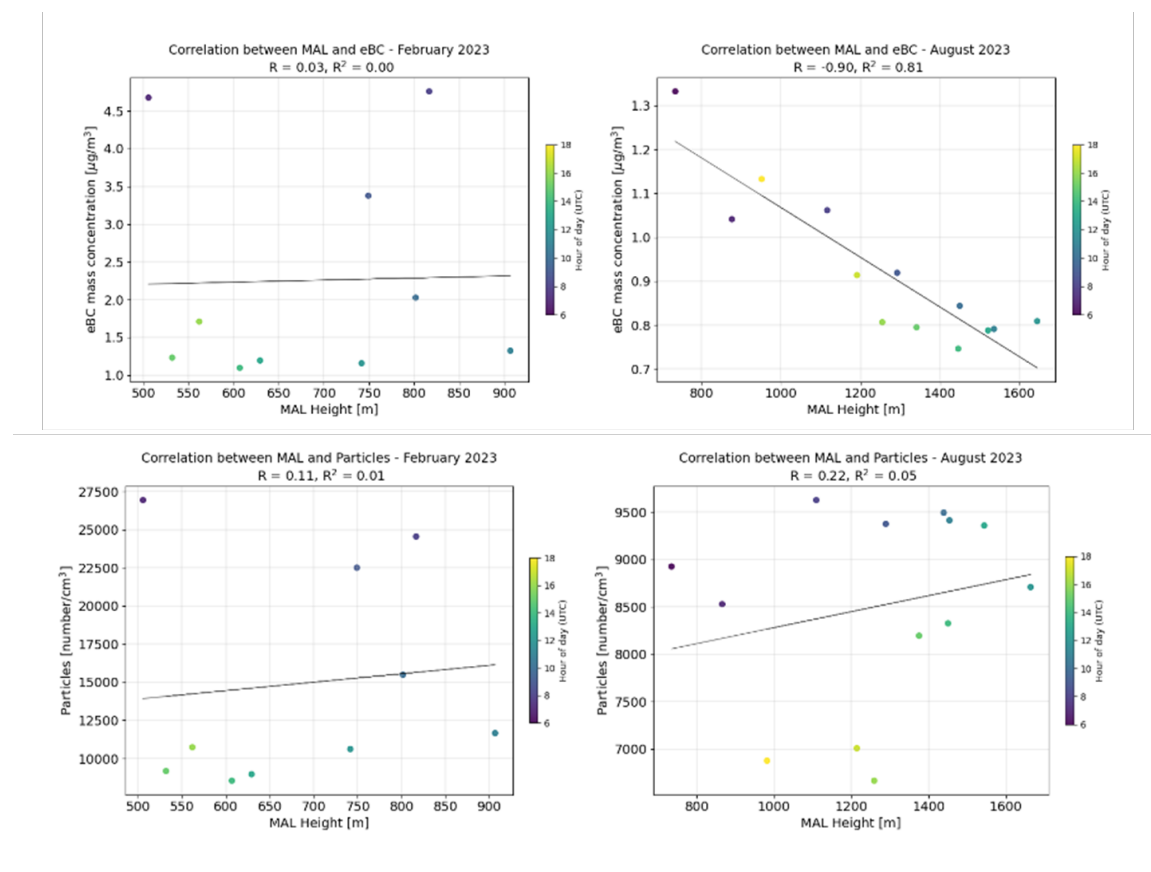


Figure 9 Example of correlation of the mixed aerosol layer height with equivalent black carbon mass concentration and with total particle number concentration in winter (top) and summer (bottom)

5.2 Export of pollution at high altitude

We here combine the data products equivalent black carbon concentration (m_{eBC}) and the height of the planetary boundary layer (PBLH) on the long-term dataset spanning from 2002 to 2023 and interesting the measurements and reanalysis data, averaged on a monthly interval Figure 10. m_{eBC} shows a strong seasonal cycle since 2002, with year-to-year variability and a net decrease in concentrations until 2016, after which a slight increasing trend was observed. Similarly, the planetary boundary layer height (PBLH) exhibits a pronounced seasonal cycle in the monthly averaged maxima, with values regularly exceeding the altitude of Monte Cimone. However, no statistically significant trends were observed in the height of the PBL over the study period.

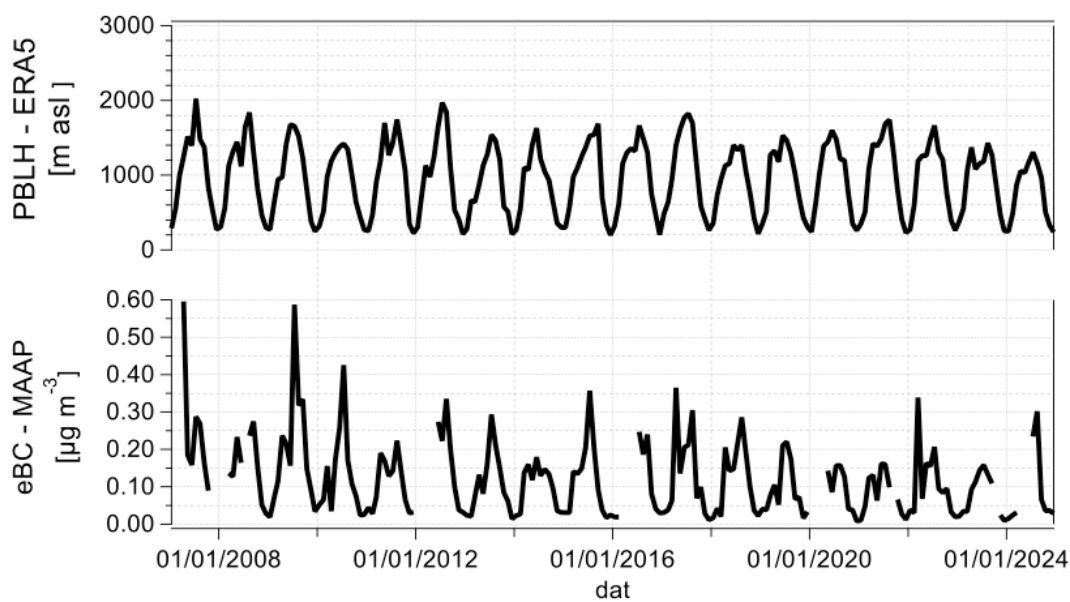


Figure 10 Monthly time series of: the equivalent black carbon mass concentration (eBC) measured at Cimone Station; height of the planetary boundary layer (PBLH) derived from ERA5 reanalysis data over the Po Valley.

Instead of focusing on the diurnal variability of eBC and PBLH, we used the long time series to examine the seasonal cycle, which appears to be clearly in phase (Figure 11). m_{eBC} increases from January to July–August, when it reaches its yearly maximum, peaking around $0.3 \mu\text{g m}^{-3}$. Lower concentrations are observed during the winter months, with values well below $0.1 \mu\text{g m}^{-3}$. This marked seasonality likely reflects several factors, including atmospheric dynamic processes and, in particular, the position of the boundary layer. Colder conditions in winter lead to a general lowering of the PBL, which barely exceeds 500 m a.s.l. during winter months. On one hand, this creates favorable conditions for pollution accumulation within the boundary layer, worsening air quality in the Po Valley. On the other hand, the low altitude of the PBL helps keep Monte Cimone isolated from the Po Valley's direct influence. Although on average between 2007 and 2023 the monthly mean of the daily maximum PBLH never exceeds the altitude of Monte Cimone, deeper PBLs—reaching up to around 2000 m a.s.l.—represent one of the main mechanisms for pollutant transport to the station. Therefore, we analyzed daily data of both PBLH and m_{eBC} to quantify their potential correlation, following the approach applied in Milan. For this analysis, we

considered only daily values of PBL height and eBC between 10:00 and 16:00. This time window focuses the dataset on the period of highest PBL development across all seasons. The monthly averaged correlation between PBLH and meBC is clearly positive (Figure 12), in contrast to what is observed in Milan. This preliminary application of the dataset indicates a strong influence of boundary layer dynamics on long-term black carbon variability, where deep boundary layers promote vertical export of pollutants from the Po Valley to higher altitudes. Future work may include the identification of climate-related anomalies using the nearly twenty-year record.

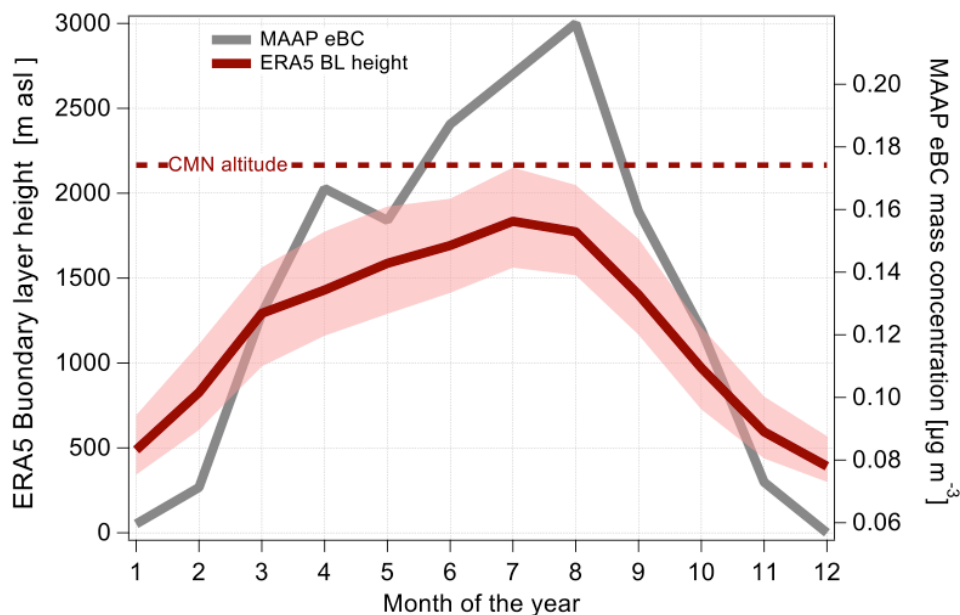


Figure 11 Seasonal cycle of the equivalent black carbon mass concentration (eBC) measured at Cimone Station; height of the planetary boundary layer (PBLH) derived from ERA5 reanalysis data over the Po Valley.

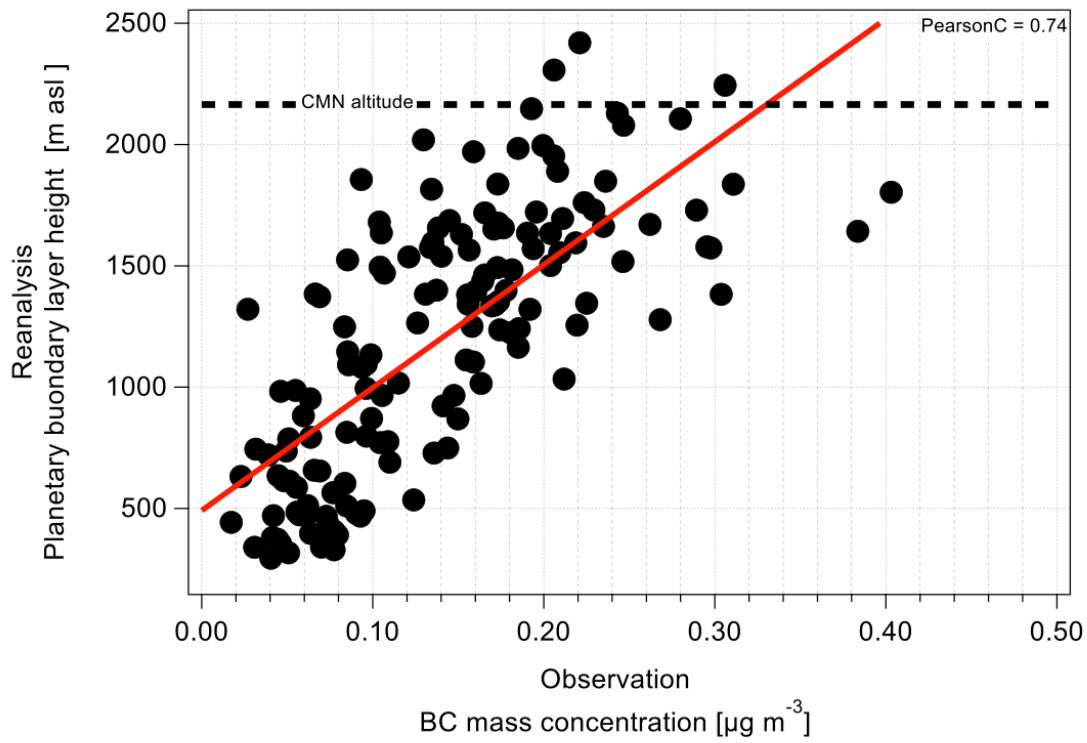


Figure 12 Correlation between the observed equivalent black carbon mass concentration and height of the planetary boundary layer at the Cimone observatory.

6 REFERENCES

Bellini, A., Diémoz, H., Di Liberto, L., Gobbi, G. P., Bracci, A., Pasqualini, F., and Barnaba, F.: Alicenet – An Italian network of Automated Lidar-Ceilometers for 4D aerosol monitoring: infrastructure, data processing, and applications, *EGUsphere*, 1–47, <https://doi.org/10.5194/egusphere-2024-730>, 2024.

Bellini, A., Diémoz, H., Gobbi, G. P., Di Liberto, L., Bracci, A., and Barnaba, F.: Aerosols in the Mixed Layer and Mid-Troposphere from Long-Term Data of the Italian Automated Lidar-Ceilometer Network (ALICENET) and Comparison with the ERA5 and CAMS Models, *Remote Sens.*, 17, 372, <https://doi.org/10.3390/rs17030372>, 2025.

Bozzo, A., Remy, S., Benedetti, A., Flemming, J., Bechtold, P., Rodwell, M., and Morcrette, J. J.: Implementation of a CAMS-based aerosol climatology in the IFS, ECMWF, 2017.

Cristofanelli, P., Bonasoni, P., Carboni, G., Calzolari, F., Casarola, L., Zauli Sajani, S., and Santaguida, R.: Anomalous high ozone concentrations recorded at a high mountain station in Italy in summer 2003, *Atmos. Environ.*, 41, 1383–1394, <https://doi.org/10.1016/j.atmosenv.2006.10.017>, 2007.

Cristofanelli, P., Marinoni, A., Arduini, J., Bonafè, U., Calzolari, F., Colombo, T., Decesari, S., Duchi, R., Facchini, M. C., Fierli, F., Finessi, E., Maione, M., Chiari, M., Calzolari, G., Messina, P., Orlandi, E., Roccato, F., and Bonasoni, P.: Significant variations of trace gas composition and aerosol properties at Mt. Cimone during air mass transport from North Africa – contributions from wildfire emissions and mineral dust, *Atmospheric Chem. Phys.*, 9, 4603–4619, <https://doi.org/10.5194/acp-9-4603-2009>, 2009.

Cristofanelli, P., Fierli, F., Marinoni, A., Calzolari, F., Duchi, R., Burkhardt, J., Stohl, A., Maione, M., Arduini, J., and Bonasoni, P.: Influence of biomass burning and anthropogenic emissions on ozone, carbon monoxide and black carbon at the Mt. Cimone GAW-WMO global station (Italy, 2165 m a.s.l.), *Atmospheric Chem. Phys.*, 13, 15–30, <https://doi.org/10.5194/acp-13-15-2013>, 2013.

Cristofanelli, P., Scheel, H.-E., Steinbacher, M., Saliba, M., Azzopardi, F., Ellul, R., Fröhlich, M., Tositti, L., Brattich, E., Maione, M., Calzolari, F., Duchi, R., Landi, T. C., Marinoni, A., and Bonasoni, P.: Long-term surface ozone variability at Mt. Cimone WMO/GAW global station (2165 m a.s.l., Italy), *Atmos. Environ.*, 101, 23–33, <https://doi.org/10.1016/j.atmosenv.2014.11.012>, 2015.

Cristofanelli, P., Brattich, E., Decesari, S., Landi, T. C., Maione, M., Putero, D., Tositti, L., and Bonasoni, P.: Aerosol Chemical Composition at the Mt. Cimone WMO/GAW Global Station, in: *High-Mountain Atmospheric Research: The Italian Mt. Cimone WMO/GAW Global Station (2165 m a.s.l.)*, edited by: Cristofanelli, P., Brattich, E., Decesari, S., Landi, T. C., Maione, M., Putero, D., Tositti, L., and Bonasoni, P., Springer International Publishing, Cham, 99–118, https://doi.org/10.1007/978-3-319-61127-3_5, 2018.

Duchi, R., Cristofanelli, P., Landi, T. C., Arduini, J., Bonafè, U., Bourcier, L., Busetto, M., Calzolari, F., Marinoni, A., Putero, D., and Bonasoni, P.: Long-term (2002–2012)

investigation of Saharan dust transport events at Mt. Cimone GAW global station, Italy (2165 m a.s.l.), *Elem. Sci. Anthr.*, 4, 000085, <https://doi.org/10.12952/journal.elementa.000085>, 2016.

Hersbach, H., Bell, B., Berrisford, P., Hirahara, S., Horányi, A., Muñoz-Sabater, J., Nicolas, J., Peubey, C., Radu, R., Schepers, D., Simmons, A., Soci, C., Abdalla, S., Abellan, X., Balsamo, G., Bechtold, P., Biavati, G., Bidlot, J., Bonavita, M., De Chiara, G., Dahlgren, P., Dee, D., Diamantakis, M., Dragani, R., Flemming, J., Forbes, R., Fuentes, M., Geer, A., Haimberger, L., Healy, S., Hogan, R. J., Hólm, E., Janisková, M., Keeley, S., Laloyaux, P., Lopez, P., Lupu, C., Radnoti, G., de Rosnay, P., Rozum, I., Vamborg, F., Villaume, S., and Thépaut, J.-N.: The ERA5 global reanalysis, *Q. J. R. Meteorol. Soc.*, 146, 1999–2049, <https://doi.org/10.1002/qj.3803>, 2020.

Inness, A., Ades, M., Agustí-Panareda, A., Barré, J., Benedictow, A., Blechschmidt, A.-M., Dominguez, J. J., Engelen, R., Eskes, H., Flemming, J., Huijnen, V., Jones, L., Kipling, Z., Massart, S., Parrington, M., Peuch, V.-H., Razinger, M., Remy, S., Schulz, M., and Suttie, M.: The CAMS reanalysis of atmospheric composition, *Atmospheric Chem. Phys.*, 19, 3515–3556, <https://doi.org/10.5194/acp-19-3515-2019>, 2019.

Israelevich, P., Ganor, E., Alpert, P., Kishcha, P., and Stupp, A.: Predominant transport paths of Saharan dust over the Mediterranean Sea to Europe, *J. Geophys. Res. Atmospheres*, 117, <https://doi.org/10.1029/2011JD016482>, 2012.

Marenco, F., Bonasoni, P., Calzolari, F., Ceriani, M., Chiari, M., Cristofanelli, P., D'Alessandro, A., Fermo, P., Lucarelli, F., Mazzei, F., Nava, S., Piazzalunga, A., Prati, P., Valli, G., and Vecchi, R.: Characterization of atmospheric aerosols at Monte Cimone, Italy, during summer 2004: Source apportionment and transport mechanisms, *J. Geophys. Res. Atmospheres*, 111, 2006JD007145, <https://doi.org/10.1029/2006JD007145>, 2006.

Marinoni, A., Cristofanelli, P., Calzolari, F., Roccatò, F., Bonafè, U., and Bonasoni, P.: Continuous measurements of aerosol physical parameters at the Mt. Cimone GAW Station (2165 m asl, Italy), *Sci. Total Environ.*, 391, 241–251, <https://doi.org/10.1016/j.scitotenv.2007.10.004>, 2008.

MedECC: Climate and Environmental Change in the Mediterranean Basin – Current Situation and Risks for the Future. First Mediterranean Assessment Report, Zenodo, <https://doi.org/10.5281/ZENODO.7224821>, 2020.

Morcrette, J.-J., Boucher, O., Jones, L., Salmond, D., Bechtold, P., Beljaars, A., Benedetti, A., Bonet, A., Kaiser, J. W., Razinger, M., Schulz, M., Serrar, S., Simmons, A. J., Sofiev, M., Suttie, M., Tompkins, A. M., and Untch, A.: Aerosol analysis and forecast in the European Centre for Medium-Range Weather Forecasts Integrated Forecast System: Forward modeling, *J. Geophys. Res. Atmospheres*, 114, <https://doi.org/10.1029/2008JD011235>, 2009.

Müller, T., Henzing, J. S., De Leeuw, G., Wiedensohler, A., Alastuey, A., Angelov, H., Bizjak, M., Collaud Coen, M., Engström, J. E., Gruening, C., Hillamo, R., Hoffer, A., Imre, K., Ivanow, P., Jennings, G., Sun, J. Y., Kalivitis, N., Karlsson, H., Komppula, M., Laj, P.,

Li, S.-M., Lunder, C., Marinoni, A., Martins Dos Santos, S., Moerman, M., Nowak, A., Ogren, J. A., Petzold, A., Pichon, J. M., Rodriguez, S., Sharma, S., Sheridan, P. J., Teinilä, K., Tuch, T., Viana, M., Virkkula, A., Weingartner, E., Wilhelm, R., and Wang, Y. Q.: Characterization and intercomparison of aerosol absorption photometers: result of two intercomparison workshops, *Atmospheric Meas. Tech.*, 4, 245–268, <https://doi.org/10.5194/amt-4-245-2011>, 2011.

Pisso, I., Sollum, E., Grythe, H., Kristiansen, N. I., Cassiani, M., Eckhardt, S., Arnold, D., Morton, D., Thompson, R. L., Groot Zwaafink, C. D., Evangeliou, N., Sodemann, H., Haimberger, L., Henne, S., Brunner, D., Burkhardt, J. F., Fouilloux, A., Brioude, J., Philipp, A., Seibert, P., and Stohl, A.: The Lagrangian particle dispersion model FLEXPART version 10.4, *Geosci. Model Dev.*, 12, 4955–4997, <https://doi.org/10.5194/gmd-12-4955-2019>, 2019.

Slowik, J. G., Cross, E. S., Han, J.-H., Davidovits, P., Onasch, T. B., Jayne, J. T., Williams, L. R., Canagaratna, M. R., Worsnop, D. R., Chakrabarty, R. K., Moosmüller, H., Arnott, W. P., Schwarz, J. P., Gao, R.-S., Fahey, D. W., Kok, G. L., and Petzold, A.: An Inter-Comparison of Instruments Measuring Black Carbon Content of Soot Particles, *Aerosol Sci. Technol.*, 41, 295–314, <https://doi.org/10.1080/02786820701197078>, 2007.

Zanatta, M., Gysel, M., Bukowiecki, N., Müller, T., Weingartner, E., Areskoug, H., Fiebig, M., Yttri, K. E., Mihalopoulos, N., Kouvarakis, G., Beddows, D., Harrison, R. M., Cavalli, F., Putaud, J. P., Spindler, G., Wiedensohler, A., Alastuey, A., Pandolfi, M., Sellegri, K., Swietlicki, E., Jaffrezo, J. L., Baltensperger, U., and Laj, P.: A European aerosol phenomenology-5: Climatology of black carbon optical properties at 9 regional background sites across Europe, *Atmos. Environ.*, 145, 346–364, <https://doi.org/10.1016/j.atmosenv.2016.09.035>, 2016.